The Photochemical Spin Dynamics of the Vitamin B_{12} Derivative, Methylcobalamin

Valentina Lukinović,[†‡§∥] Jonathan R. Woodward,*[⊥] Teresa C. Marrafa,[†§] Muralidharan Shanmugam,[§] Derren J. Heyes,[§] Samantha J. O. Hardman,[§] Nigel S. Scrutton,[†§] Sam Hay,[†§] Alistair J. Fielding*[†‡∇] and Alex R. Jones*[†‡§○]

[†]School of Chemistry and [‡]Photon Science Institute, The University of Manchester, Oxford Road, Manchester, M13 9PL, UK

[§]Manchester Institute of Biotechnology, The University of Manchester, 131 Princess Street, Manchester, M1 7DN, UK

[⊥]Graduate School of Arts and Sciences, The University of Tokyo, 3-8-1 Komaba, Meguro-ku, Japan

[∥]Present Address: Institute for Advanced Biosciences, Research Centre UGA, Health Site – Allée des Alpes, 38700, La Tronche, France

[∇]Present Address: School of Pharmacy and Biomolecular Sciences, Liverpool John Moores University, James Parsons Building, Byrom Street, Liverpool, L3 3AF, UK

[○]Present Address: National Physical Laboratory, Hampton Road, Teddington, Middlesex, TW11 0LW, UK

ABSTRACT: Derivatives of vitamin B_{12} are six-coordinate cobalt corrinoids found in humans, other animals and micro-organisms. By acting as enzymatic cofactors and photoreceptor chromophores they serve vital metabolic and photoprotective functions. Depending on the context, the chemical mechanisms of the biologically-active derivatives of B_{12} – methylcobalamin (MeCbl) and 5'-deoxyadenosylcobalamin (AdoCbl) – can be very different from one another. The extent to which this chemistry is tuned by the upper axial ligand, however, is not yet clear. Here, we have used a combination of time-resolved FT-EPR, magnetic field effect experiments and spin dynamic simulations to reveal that the upper axial ligand alone only results in relatively minor changes to the photochemical spin dynamics of B_{12}. By studying the photolysis of MeCbl, we find that, much like for AdoCbl, the initial (or 'geminate') radical pairs are born predominantly in the singlet spin-state and thus originate from singlet excited-state precursors. This is in contrast to the triplet radical pairs and precursors proposed previously. Unlike AdoCbl, the extent of geminate recombination is limited following MeCbl photolysis, resulting in significant distortions to the FT-EPR signal caused by polarization from spin-correlated methyl-methyl radical 'f-pairs' formed following rapid diffusion. Despite the photophysical mechanism that precedes photolysis of MeCbl showing a wavelength-dependence, the subsequent spin dynamics appear to be largely independent of excitation wavelength, again much like for AdoCbl. Our data finally provide clarity to what in the literature to date has been a confused and contradictory picture. We conclude that, although the upper axial position of MeCbl and AdoCbl does impact their reactivity to some extent, the remarkable biochemical diversity of these fascinating molecules is most likely a result of tuning by their protein environment.

INTRODUCTION

Vitamin B_{12} is vital to the healthy function of both animals and microbes,[1] and its deficiency in humans can lead to potentially serious haematological and neuropsychiatric disorders.[2] It belongs to a family of six-coordinate cobalt corrinoid macrocycles known as the cobalamins.[3] In the biologically active cobalamin derivatives, the lower axial position is usually occupied by the 5,6-dimethylbenzimidazole substituent from the corrin ring, whereas the upper axial position is variable (Figure 1A). The best-described role of these derivatives is as cofactors to various metabolic enzymes,[4] whose activation mechanism depends on the identity of the upper-axial ligand. Methylcobalamin (MeCbl) is a methyltransferase[5] coenzyme where, upon substrate binding, the covalent Co–C bond to the methyl breaks heterolytically, converting Co^{III} to Co^{I} and transferring a methyl cation to the substrate. By contrast, upon substrate binding to B_{12}-dependent mutase[6] and eliminase[7] enzymes, the Co–C bond in 5'-deoxyadenosylcobalamin (AdoCbl) breaks homolytically, producing a 5'-deoxyadenosyl-cob(II)alamin radical pair (RP) and triggering radical-mediated catalysis. It is still not clear to what extent the upper axial ligand tunes cobalamin reactivity.

B_{12} derivatives can also undergo extensive photochemistry.[8] This sensitivity to light was first observed shortly after their discovery,[9] and has since been used to investigate the electronic structure of cobalamins with different upper-axial ligands,[8, 10-22] and how this structure and the protein environment[23-27] influences their reactivity. In recent years, both AdoCbl and MeCbl have also been discovered to have roles as chromophores to light-activated, bacterial transcriptional regulators.[8, 28-35] As with its enzymatic activation, the photoexcitation of AdoCbl free in solution leads to the 5'-deoxyadenosyl-

cob(II)alamin RP (Figure 1B). The RP is singlet (S)-born,[36] produced with near unity quantum yield,[20] and this fate appears to be independent of the excitation wavelength.[17] Unlike its enzymatic activation, the photolysis of free MeCbl also generates a RP (methyl-cob(II)alamin). The photophysical pathway leading to radicals (Figure 1C), however, is more complex than that of AdoCbl. Transient absorption experiments have revealed that two photodissociation pathways are possible at around physiological pH, the relative extent of which is dependent on the excitation wavelength.[17] After photoexcitation at 530 nm, for example, most excited molecules relax to a metal-to-ligand charge transfer-like S_1 state, from which 85% relax back to the ground state and 15% form RPs. If higher excited states are initially populated, however, (e.g., by photoexcitation at ~ 400 nm), a population of RPs is produced directly from these higher states (e.g., with a yield of ~ 25% at 400 nm). The remaining population relaxes to the S_1 state, which then non-radiatively decays to the ground state or forms RPs as before.

The differences in photoresponse of MeCbl and AdoCbl have the strong potential to inform on how the chemistry of cobalamins is tuned by their ligation and protein environment. This potential is currently being severely limited, however, by the significant confusion in the literature about the multiplicity of the RP precursors following photoexcitation of MeCbl. Magnetic field effect (MFE) data suggest that, like AdoCbl, MeCbl RPs are S-born.[24, 37] Conservation of spin means that the RP precursors are therefore also in a S excited state. By contrast, chemically induced dynamic electron polarization (CIDEP) electron paramagnetic resonance (EPR) signals following the photolysis of both MeCbl[36, 38] and its analogue, methylaquocobaloxime,[39] have been interpreted to originate from triplet mechanism (TM) polarization (section 2.1.1. Supporting Information). Triplet (T)-born RPs are consistent with initial time-dependent density functional theory (TD-DFT) calculations, which claimed that photolysis of the Co–C bond in MeCbl is mediated by a repulsive T-state.[40] Later TD-DFT from the same group, however, appeared to reconcile with the MFE data, indicating that intersystem crossing to the T-excited state is likely to have a low probability, implying that the RP precursors are indeed S.[41] To add further to the confusion, Bussandri *et al.*[36] argue that their CIDEP data might be explained by either T-born RPs and ST_0 spin-state interconversion or S-born RPs and ST_{-1} interconversion (section 2.1.2 Supporting Information). All such assignments are rather speculative, however, as none of the EPR studies to date have been supported by spin dynamic simulations.

Herein, we use a combination of time-resolved Fourier transform-EPR (FT-EPR), MFE experiments and spin dynamic simulation to provide the first comprehensive description of the photochemical spin-dynamics of MeCbl at neutral pH. The data reveal that, like AdoCbl, geminate methyl-cob(II)alamin RPs (i.e., those formed immediately following bond homolysis) are S-born following photoexcitation and that this multiplicity appears to be independent of excitation wavelength. Spin polarization from these S-born geminate pairs is combined with significant polarization from spin correlated methyl-methyl RPs following the random encounter of freely diffusing radicals (known as 'f-pairs').

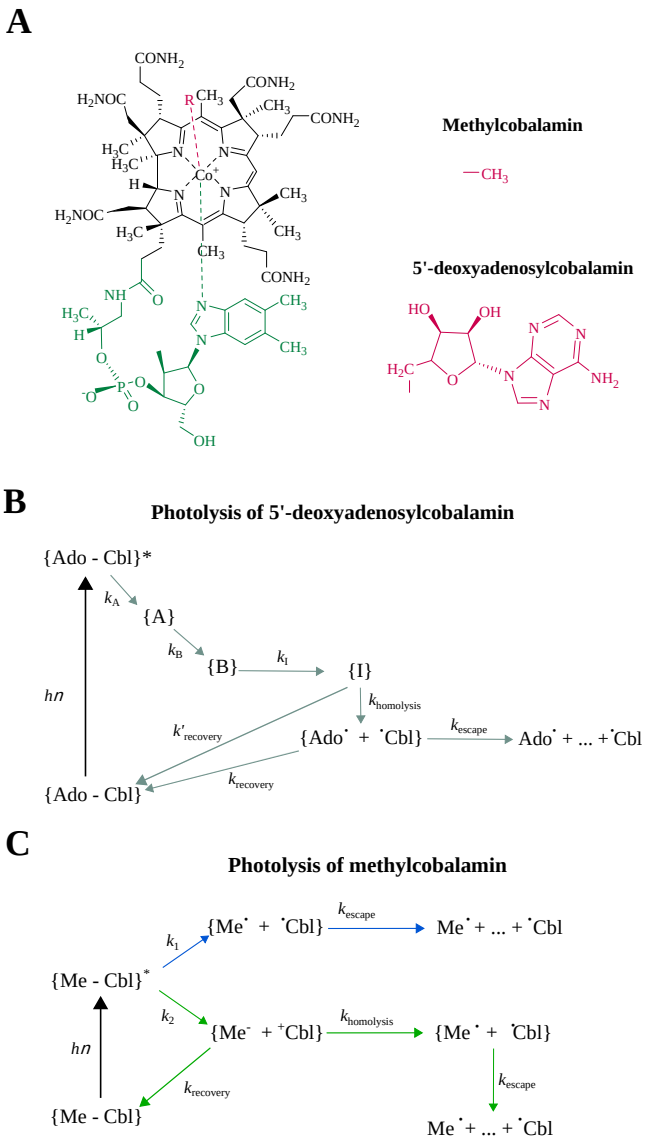

Figure 1. (A) Structure of cobalamin with methyl and 5'-deoxyadenosyl as upper axial ligands *('R', pink)* and 5,6-dimethylbenzimidazole as lower axial ligand *(green)*. Schematic diagrams displaying photophysical and photochemical dynamics of AdoCbl (B) and MeCbl (C). The photoresponse of AdoCbl is independent of excitation wavelength, whereas MeCbl has been shown to depend on the excitation wavelength (blue and green arrows, panel C – see main text for discussion). Ado˙+˙Cbl – 5'-deoxyadenosyl-cob(II)alamin RP; Me˙+˙Cbl – methyl-cob(II)alamin RP; RPs in brackets are within the solvent cage, those without are solvent-separated; {Me-+⁺Cbl}[31, 34] – metal-to-ligand charge transfer state. {A}, {B} and {I} in panel B represent short-lived intermediates, with k_A, k_B and k_I their rates of formation. k_1 and k_2 in panel C are rates of formation of the 'prompt' RP and metastable photoproduct, respectively. In both B and C: k_{escape} – rate of escape from the solvent cage; $k_{homolysis}$ – rate of Co–C homolysis; $k_{recovery}$ – rate of non-radiative recovery to the ground state. Adapted from Shiang *et al.*[17]

RESULTS AND DISCUSSION

The methyl radical signal contains polarization from both geminate RPs and those formed following diffusive encounter

All time-resolved FT-EPR experiments were conducted using a continuous-flow cell built in-house (details in Supporting Information, Section 1, Scheme S1 and Figures S1&2). First, measurements of methyl radicals were conducted at 9 GHz following photoexcitation of MeCbl at 532 nm in aqueous buffer. At room temperature, only the methyl radical is detectable using FT-EPR owing to the fast relaxation of the cob(II)alamin radical.[42] Example spectra at five different delays-after-flash (DAF) are shown in Figure 2A. The measured hyperfine coupling of 2.26 mT is in agreement with previously published data for the methyl radical.[36, 43] Initially, the photochemically generated RPs are spin polarized, and the spectra in Figure 2A therefore deviate from the 1:3:3:1 pattern expected for a population of methyl radicals at thermal equilibrium. The spectra exhibit 4 resonance lines that are all in absorption with the high field lines enhanced compared to the low field side. This high to low field distortion increases with increasing DAF, and the lowest field resonance line ultimately begins to change from an absorptive to an emissive signal at DAF = 360 ns.

To investigate the origin of this spin polarization and its evolution with time, attempts were made to simulate the data in Figure 2A by combining the polarization patterns for the methyl radical generated through the following possible polarization mechanisms (Figure 2B):

1) Absorptive triplet mechanism (TM)
2) Emissive TM
3) S-born ST_0 radical pair mechanism (RPM)
4) T-born ST_0 RPM
5) S-born ST_{-1} RPM (including net effect from the cob(II)alamin radical)
6) T-born ST_{-1} RPM (including net effect from the cob(II)alamin radical).

For full details of the simulation procedure refer to Section 2 and Figure S3 of the Supporting Information. We found that no combination of the above polarization patterns is capable of reproducing the polarization patterns observed in Figure 2A (e.g., Figure S4). TM polarization arises from selective population of T excited states during intersystem crossing in the RP precursor, which is then transferred to the radicals.[44-45] The result is polarization very close to the 1:3:3:1 ratio produced by equilibrium polarization. Depending on which T sub-levels are populated during intersystem crossing, this polarization is either entirely absorptive (Figure 2B.1) or entirely emissive (Figure 2B.2) and lacks any of the high to low field distortion we observe. In many observations of CIDEP, RPM polarization gives rise to low field emissive/high field absorptive (E/A) or A/E polarization patterns. In this system, however, the very large difference in g-values between the methyl and cob(II)alamin radicals means that all of the RPM polarization patterns are also close to the 1:3:3:1 ratio (Figures 2B.3-6).[36]

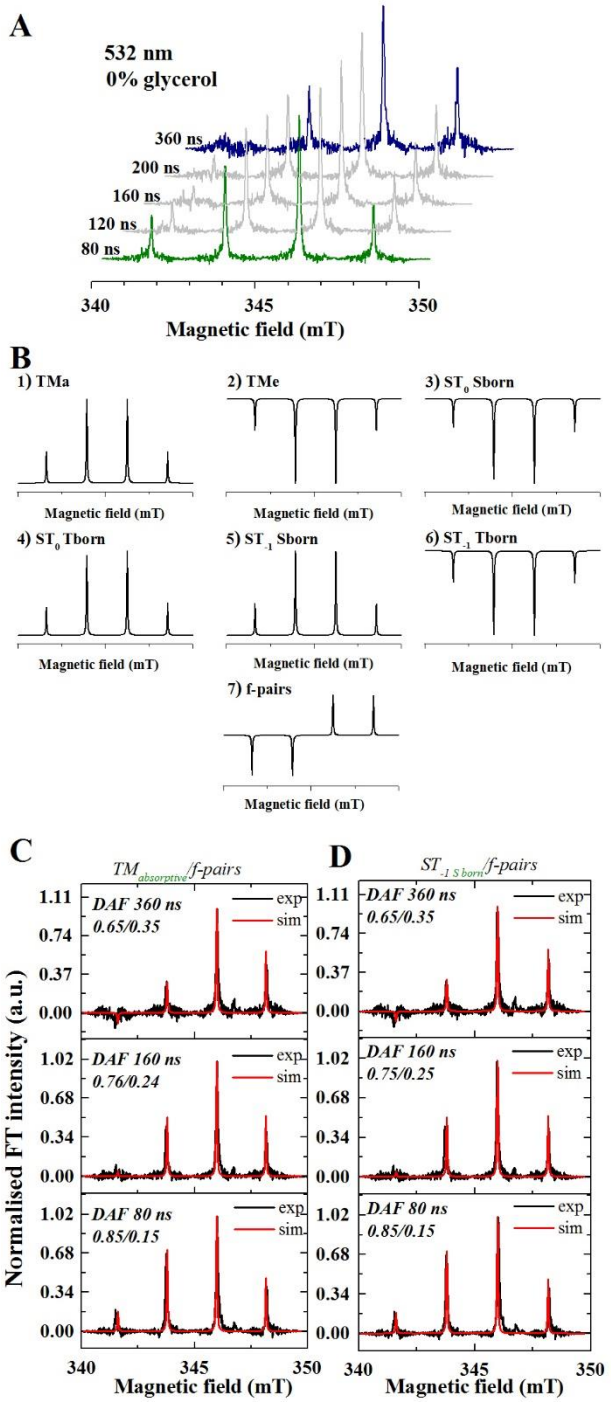

Figure 2. (A) FT-EPR spectra of the methyl radical at five different DAF following photoexcitation of MeCbl at 532 nm. (B) Theoretical spectra for the methyl radical from different spin polarization mechanisms. The negative hyperfine value for the methyl radical is taken into account. TM - triplet mechanism; subscript a – absorptive; subscript e - emissive; RPM - radical pair mechanism, originating from mixing of S and T_0 or S and T_{-1} states and each from T-born or S-born pairs. Simulation of FT-EPR spectra using a combination of absorptive TM / methyl-methyl f-pairs (C) and $ST_{-1\ S\text{-}born}$ RPM / methyl-methyl f-pairs (D). Fractional contributions from

each form of polarization is stated within each panel. All data were acquired in aqueous buffer at room temperature.

Another source of spin polarization is therefore necessary to explain the observed FT-EPR spectra and their time dependence. Considering likely dynamic processes and given the need for a substantial difference in the intensity of the two low field lines relative to the two high field lines, we propose that key to the observed polarization is the involvement of freely diffusing pairs (f-pairs) consisting of two methyl radicals from two distinct precursor molecules. Such f-pairs have no difference in g-values; therefore ST_0 RPM polarization patterns exhibit the familiar E/A pattern (Figure 2B.7). Using any absorptive 1:3:3:1 polarization pattern (Figures 2B.1, 4 & 5) in combination with increasing proportions of f-pair polarization allows all observed spectra to be simulated with good accuracy (Figures 2C&D and S5-8). For clarity, signal intensities for the data and simulations in Figures 2C&D are also plot as bar charts with error bars in Figures S9A&B, respectively. The fact that this distortion increases with time is also consistent with polarization from f-pairs, which form following diffusion of the methyl radicals away from the geminate pairs. We therefore hypothesized at this stage that the magnitude of f-pair polarization increased with DAF. We will address this in greater detail below.

The majority of geminate RPs created following photolysis of MeCbl are S-born

First, we investigated the question of the correct source of the initial, absorptive pattern that is close to the 1:3:3:1 ratio. As the spectra in Figure 2B indicate, this can have three possible origins:

1) Absorptive TM
2) T-born ST_0 RPM
3) S-born ST_{-1} RPM

where 1) and 2) can, in principle, both be generated by the same T-born RPs. Because of the similarity between the three patterns, there is no way to determine unequivocally which of these mechanisms are responsible from the FT-EPR spectra alone. That said, given the large hyperfine couplings of the cob(II)alamin radical, ST_{-1} RPM polarization is expected to be large and readily observable in this reaction.[36] It is therefore possible to simulate the observed spectra using only S-born geminate RPs, which would be consistent with existing MFE data[24, 37] and the most recent TD-DFT calculations.[41] In further support for this assignment is the fact that TM polarization observed in the MeCbl analogue, methylaquocobaloxime, is emissive[39] rather than absorptive.

To investigate further we analyzed the magnetic sensitivity of MeCbl photolysis, which again is consistent with predominantly S-born RPs (Figure 3). In previous MFE studies with MeCbl, we conducted both photolysis and detection within a stopped-flow spectrophotometer using white light illumination from a Xe arc lamp.[24] Using a similar experimental setup adapted to better align with the FT-EPR experiments, here we continuously illuminated a viscous, aqueous solution (50% glycerol) of MeCbl using a 530 nm LED under anaerobic conditions and exposure to a 100 mT magnetic field. Throughout, accumulation of the cob(II)alamin radical was monitored as a function of time using light from the arc lamp monochromated to 470 nm. These data (Figure 3A) show that less cob(II)alamin accumulates as a function of time when the system is exposed to 100 mT, and are therefore consistent with magnetically-sensitive RPs being predominantly S-born (Figure 3B). In zero applied field the S-born methyl-cob(II)alamin RP can efficiently interconvert with all three T RP spin-states, none of which can

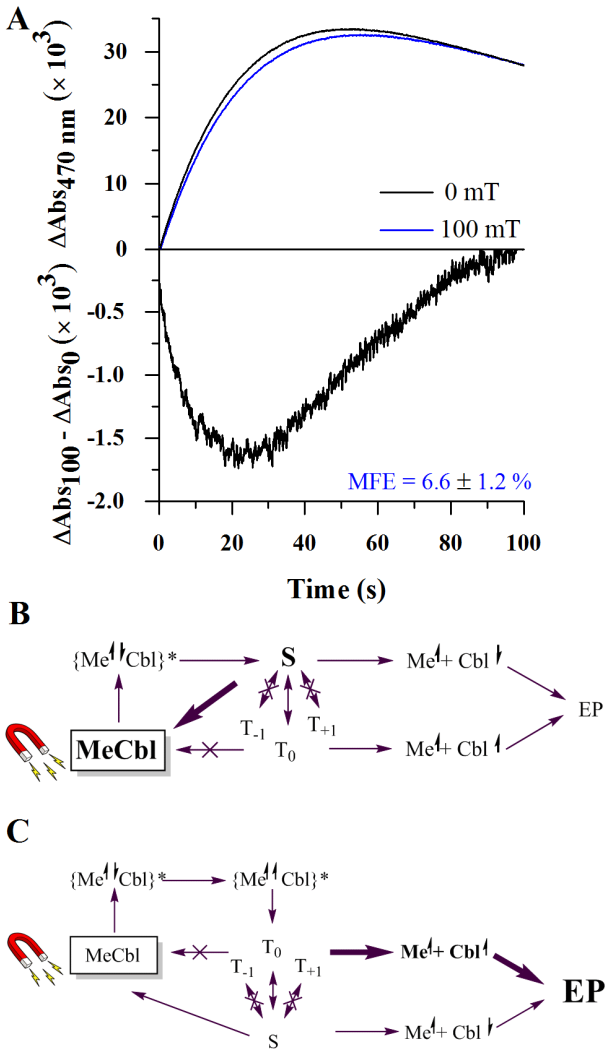

Figure 3. (A) Continuous-wave photolysis of MeCbl in an anaerobic, aqueous solution of 50% glycerol using a 530 nm LED. Top plot: accumulation of the cob(II)alamin radical was monitored by following the absorption at 470 nm in the absence (black) and presence (blue) of a 100 mT magnetic field. Bottom plot: the magnitude of the magnetic field effect (MFE) is illustrated by subtracting the ΔAbs(0 mT) from ΔAbs(100 mT). The percentage MFE was estimated to be 6.6 ± 1.2% by dividing the ΔAbs(0 mT) by the peak ΔAbs(100 mT) – ΔAbs(0 mT) at the corresponding time point. Schemes illustrating the predicted effects of a 100 mT magnetic field on the RP reaction dynamics following the photolysis of MeCbl if the methyl-cob(II)alalmin RP were S-born (B) or T-born (C). The yield of escape products (EP; i.e., cob(II)alamin) is higher for T-born RPs exposed to a 100 mT magnetic field than for S-born pairs under the same conditions. See main text for full discussion.

recombine to the ground state. A 100 mT magnetic field saturates the Zeeman effect of this RP,[24] in which case the S spin-state can only interconvert with the T_0 spin state. The relative population of S RPs is therefore higher for a S-born RP exposed to 100 mT compared to zero applied field and hence the probability of recombination is greater. Hence less escape product (in this case the cob(II)alamin radical) accumulates, as we observe in Figure 3A. By contrast, for a T-born RP the saturation of the Zeeman effect by a 100 mT magnetic field would instead trap the $T_{\pm1}$ RP spin-states, thus increasing the T population relative to no applied field (Figure 3C). Here, the extent of recombination from S RPs would therefore decrease and the escape product yield would correspondingly increase, which we do not observe.

When viewed in combination with the FT-EPR data, the MFE data support the hypothesis that the photolysis of MeCbl following photoexcitation using green light results in predominantly S-born geminate RPs. We cannot unequivocally rule out the possibility that both singlet and triplet geminate RPs are formed as long as there is a greater total number of singlet RPs than triplet RPs. Consistent with Occam's razor, however, all subsequent simulations in this work were performed by combining different admixtures of ST_{-1} RPM polarization from S-born geminate RPs (Figure S4E) and methyl-methyl f-pairs (Figure S4G). Most spin-correlated f-pairs are by definition T-born because the encounter of freely diffusing pairs of radicals in the S spin-state results in recombination (assuming the product is a S ground state molecule). Because those that encounter as T-pairs cannot recombine, they become T-born RPs that are initially spin polarized, and which can undergo subsequent spin dynamics. We were thus able to obtain excellent fits to the experimental spectra (Figures 2D, S8 and S9), and believe these assignments resolve the existing contradictory assignments in the literature.

Both relaxation and methyl radical diffusion control the evolution of spin polarization

As stated above, the fact that the distortion of the polarization pattern in Figure 2A increases with time is, at least in principle, consistent with an increasing population of f-pairs as the data acquisition proceeds. The generation of f-pairs is a bimolecular process and therefore follows second order kinetics, which are concentration-dependent. By extension, one might expect the extent of distortion at any one point in time to be dependent on the concentration of MeCbl. We find that this is not the case. In Figure 4A, the f-pair contribution to the polarization pattern is plotted as a function of DAF for MeCbl concentrations ranging from 0.5–3 mM. This range was chosen because below 0.5 mM the signal to noise ratio is too poor to fit the data with confidence (Figure S8A) and at 3 mM the sample absorbs almost 100% of photons (Supporting Information, Section 3). Although the contribution of methyl-methyl f-pairs to the polarization pattern increases with DAF there is no significant difference between each concentration (Figures 4A and S8).

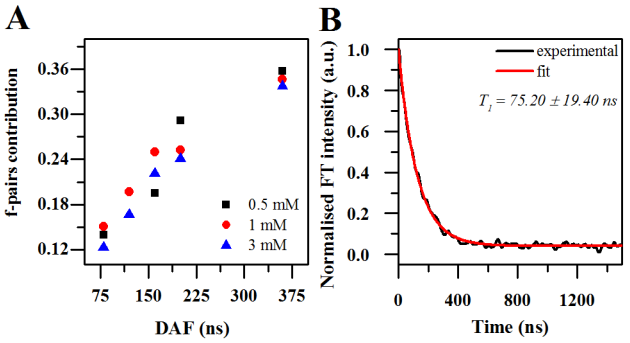

Figure 4. (A) Relative contribution of methyl-methyl f-pairs to the polarization pattern of the time-resolved FT-EPR signal as a function of [MeCbl]. (B) Example single exponential fit (red) of free induction decay at the 346 mT field position (black) to give a T_1 = 75.20 ± 19.40 ns. All data were acquired in aqueous buffer at room temperature.

Although perhaps surprising, the lack of a concentration-dependence can be explained by assessing the expected diffusion kinetics of methyl radicals. We calculated (Supporting Information, Section 4) that the approximate time required for methyl-methyl f-pair formation in aqueous solution following photolysis of MeCbl in the concentration range 0.5 – 3 mM at 532 nm varies between ~ 30 – 5 ns. The majority of f-pairs are therefore formed within the 80 ns that represents the earliest DAF we measure. Why then do we observe a time dependence of the f-pair contribution to the polarization pattern for methyl radicals? A monoexponential fit of the free induction decay following MeCbl photolysis at 532 nm in aqueous buffer gives a T_1 of 75 ± 19 ns (Figure 4B). This decay rate is consistent with the time evolution of the polarization observed in Figure 2. Thus, the observed time dependence of the f-pair contribution is predominantly because of relaxation reducing the amount of ST_{-1} RPM polarization with time relative to that from f-pairs, the absolute concentration of which remains relatively constant.

If polarization from f-pairs is pertinent, then their diffusion kinetics will have a strong dependence on solvent viscosity. We therefore hypothesized that the time evolution of the polarization pattern will change following photolysis of MeCbl in a 50% aqueous solution of glycerol. This proved to be the case (Figures 5 and S10). The polarization pattern observed here is qualitatively similar to that observed in non-viscous solution (Figure 2A), with high field enhancement. An increase in the resonance line intensities is evident (Figure 5A), presumably owing to the RP cage effect of the viscous medium. Furthermore, the spectrum at the earliest DAF of 80 ns is closer to the predicted 1:3:3:1 pattern than that observed in non-viscous solution and, although the spectral distortion increases with time, it does so to a lesser extent (Figures 5A and S10). These data are consistent with the accumulation of the distorting f-pair polarization happening more slowly in viscous solution owing to slower diffusion kinetics. This is confirmed by the now significant dependence on MeCbl concentration of the f-pair contribution to the polarization pattern (Figures 5B and S10), which is consistent with the f-pairs being formed in 50% glycerol on order of ~ 300 – 30 ns (for 0.3 – 3 mM MeCbl, respectively, Supporting Information Section 4).

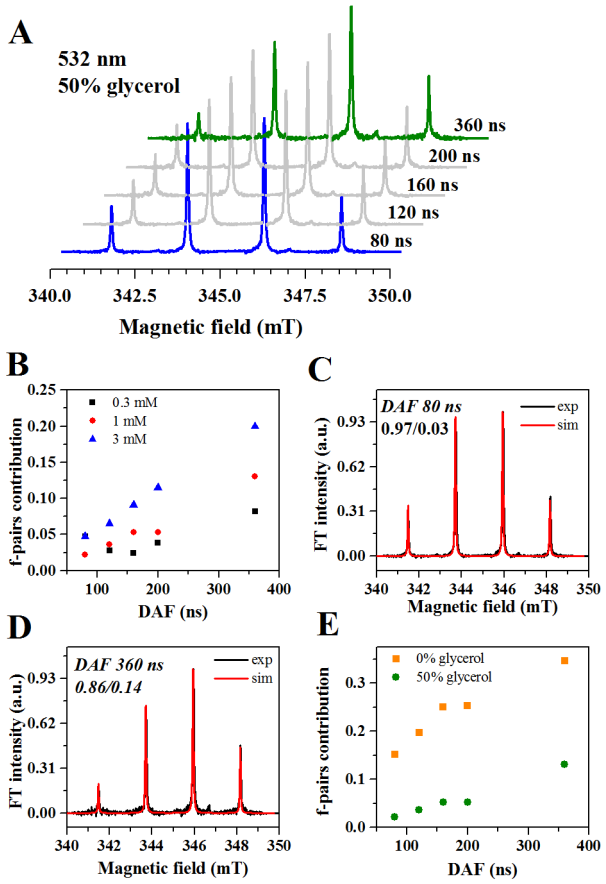

Figure 5. Unless stated otherwise, all data were acquired in an aqueous solution of 50% glycerol. (A) FT-EPR spectra of the methyl radical at five different DAF following photoexcitation of MeCbl at 532 nm. (B) Relative contribution of methyl-methyl f-pair polarization to the time-resolved FT-EPR signal at various DAF as a function of [MeCbl]. Simulation of FT-EPR spectra using a combination of ST_{-1} RPM and methyl-methyl f-pair polarization, for DAF 80 ns (C) and 360 ns (D). (E) Comparison of f-pair contribution in aqueous solution (orange) and in 50% glycerol (green).

As before, the data can be accurately simulated using a combination of ST_{-1} RPM from geminate pairs and polarization from methyl-methyl f-pairs (Figures 5C&D and S10). As expected, at high viscositythe contribution from f-pairs is lower at each time point than in aqueous solution (Figure 5E). Taken together, it is clear from these data that, in combination with slightly slower relaxation kinetics with increasing viscosity (~120 ns, Figure S11), slower diffusion of the methyl radicals now significantly contributes to the time evolution of the signal. This provides strong evidence for the contribution of methyl-methyl f-pair polarization to the methyl radical spectra following photolysis of MeCbl. It is possible that methyl-cob(II)alamin f-pairs are also formed. RPM polarization generated from such f-pairs, however, would have the same intensity pattern as the original geminate pairs and thus cannot be separated based on the extent of spectral distortion.

The spin dynamics following methylcobalamin photolysis are independent of excitation wavelength

As outlined in the introduction, after excitation at 532 nm 100% of photoexcited MeCbl molecules decay to the S_1 state before either relaxing to the ground state or generating RPs.[17, 19] By contrast, at shorter excitation wavelengths a sub-population (e.g., 25% at 400 nm) undergo homolysis directly from a higher excited state with the remaining 75% decaying to S_1 and proceeding as for excitation at 532 nm (Figure 1B).[17] The yield of RPs following excitation at shorter wavelengths is therefore greater. We initially hypothesized that the different RP precursor multiplicities proposed in the literature[36, 40-41] might be accounted for by different spin dynamics from each of these photophysical pathways. The data in Figure 6 show that this appears not to be the case. The resonance line intensities following photolysis at 355 nm of MeCbl in aqueous buffer (Figure 6A) are qualitatively similar to those observed following excitation at 532 nm (Figure 2A). Again, the data can be simulated using a combination of ST_{-1} RPM and methyl-methyl f-pair polarization patterns (Figures 6A and S12). Moreover, the spectral distortion also decreases at any particular DAF with increasing solvent viscosity (Figures 6B and S13) consistent with restricted diffusion of the methyl radicals and thus a reduced contribution to the polarization from f-pairs (Figure 6C). For clarity, the data and simulations presented in Figures 6A&B, alongside the error of the f-pair contribution, are again plot as bar charts in Figure S14.

The similarity between the spin dynamics following photoexcitation at 355 nm and 532 nm is borne out both by the FT-EPR data and by the MFE data. The extent of spectral distortion in the FT-EPR data from each excitation wavelength is almost identical (Figure 6D), as is the magnitude and phase of the MFE (Figures 3A and 6E). Both sets of data in Figures 6D&E were acquired in 50% glycerol so the conditions are consistent. Because of the faster kinetics of formation,[17] one might have expected that the RPs produced more directly from higher excited states would result in the generation of f-pairs with faster kinetics than those that are generated *via* the S_1 state. If this were the case, the geminate pair lifetime would be shorter, thus reducing the extent of ST_{-1} RPM polarization in the signal and increasing the relative f-pair contribution. Moreover, one would expect the MFE magnitude to be reduced. We observe neither of these things in our data, however, and therefore conclude that the relative contributions to the spin dynamics from geminate pairs and f-pairs at each excitation wavelength is comparable.

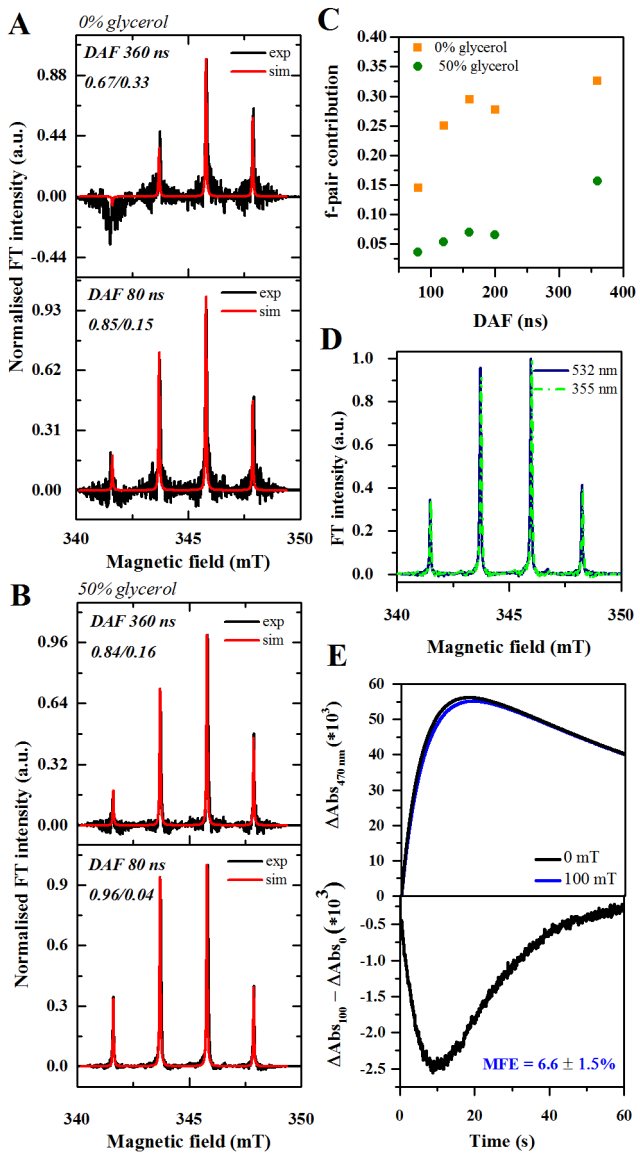

Figure 6. Overlaid experimental (black) and simulated (red) FT-EPR spectra of the methyl radical following photoexcitation of MeCbl at 355 nm at DAF = 80 and 360 ns, in aqueous buffer (A) and 50% glycerol (B). (C) Comparison of f-pair contribution in aqueous solution (orange) and 50% glycerol (green). (D) Overlaid FT-EPR spectra acquired in 50% glycerol at a DAF = 80 ns following photoexcitation at 532 (blue) and 355 nm (dashed green). (E) Effect of a 100 mT magnetic field on the accumulation of the cob(II)alamin radical following continuous wave illumination at 365 nm.

SUMMARY & CONCLUSIONS

The literature to date concerned with the photolysis of MeCbl paints a rather confused picture regarding the spin multiplicity of the resulting RPs and their precursors. Various experimental[17, 19, 24, 36-39] and theoretical[40-41, 46-48] approaches have reported evidence of either S- or T-born RPs. Different approaches of the same method have generated data consistent with different multiplicities and some of the same data sets have been interpreted as potentially consistent with either multiplicity. The data we report here from FT-EPR, MFE and spin dynamic simulations finally provides an unambiguous account of the photochemical spin dynamics of MeCbl. The recent discovery of photobiological roles for B_{12} cofactors, and their increasing application as optogenetic tools[49-50] and in light-responsive biomaterials,[51] emphasizes the importance of a clear understanding of B_{12} photochemical dynamics.

We show that several different combinations of spin polarization from both S- and T-born geminate RPs can accurately simulate the experimental FT-EPR data of the methyl radical following excitation at 532 nm. This fact might go some way to explaining much of the previous confusion in the literature. All of our simulations, however, require polarization from the formation of methyl-methyl f-pairs following radical diffusion. Only this can explain: i) the extent of distortion we observe away from the 1:3:3:1 pattern expected of the methyl radical; ii) the viscosity dependence of this spectral distortion; and iii) the spectral evolution with time at higher viscosities. Rapid diffusion of the methyl radical is consistent with previous transient absorption data, which, in contrast to AdoCbl, show little evidence of geminate, methyl-cob(II)alamin recombination in aqueous solution.[17, 52] Our MFE data are consistent with the geminate RPs being predominantly S-born. The simplest way to simulate our FT-EPR data and account for S-born geminate pairs is to combine S-born ST_{-1} RPM polarization with that from methyl-methyl f-pairs. The hyperfine couplings of the cob(II)alamin radical are very large, and ST_{-1} RPM polarization is therefore also expected to be large and readily observable in this reaction.

We initially hypothesized that, because different photophysical pathways are accessible at different excitation wavelengths for MeCbl (Figure 1C),[17] the multiplicity of the RP precursors too would be wavelength-dependent. Our FT-EPR and MFE data suggest this isn't the case. Following photoexcitation of MeCbl at both 532 and 355 nm our data are consistent with S-born geminate pairs. It was also considered possible that methyl radicals formed following prompt photolysis at 355 nm would form f-pairs both more rapidly and with higher concentrations as a function of time. In contrast to a previous report,[36] however, we did not find that the FT-EPR spectra of the methyl radical acquired following photoexcitation at 355 nm were more distorted than those acquired at 532 nm (Figure 6D). Because this distortion can only be accounted for by f-pair polarization, it therefore appears that the relative proportion of geminate and f-pairs at each wavelength is similar. This is supported by the fact that the magnitude of the MFE at each wavelength is the same within error. A greater population of f-pairs would reduce the relative proportion of magnetically-sensitive geminate pairs and hence the magnitude of the MFE on the signal.

We therefore conclude that, following photoexcitation, methyl-cob(II)alamin geminate RPs are predominantly if not entirely S-born and generate spin polarization *via* ST_{-1} RPM (Figure 7). The small methyl radical then diffuses rapidly to form methyl-methyl f-pairs. Because the methyl radicals that encounter in the S spin-state react, most likely to form ethane, the spin-correlated f-pairs that do not are by definition T-born, and generate further spin polarization *via* ST_0 RPM. Other side

reactions of the methyl radical are in principle possible, including H-abstraction from somewhere on the cobalamin or possible reactions with the solvent. Such side reactions could perhaps contribute to an apparent limit to the f-pair contributions of somewhere between 30-40% (Figures 4A, 5E & 6C). Despite the fact the photophysics following excitation of MeCbl is wavelength-dependent, the subsequent spin dynamics are largely unaffected by excitation wavelength. The photolysis of both AdoCbl and MeCbl therefore generate S-born RPs. The only significant difference in this regard is that the quantum yield of photochemically-generated RPs from AdoCbl is significantly higher,[20] and the yield of radicals from MeCbl only increases with a larger input of energy.[17] This might suggest that AdoCbl is more inclined towards radical chemistry than MeCbl. However, the fact that photolysis in solution of both forms generates RPs with similar spin dynamics suggests that it is predominantly the protein environment that tunes the reactivity of biologically active B_{12} derivatives.

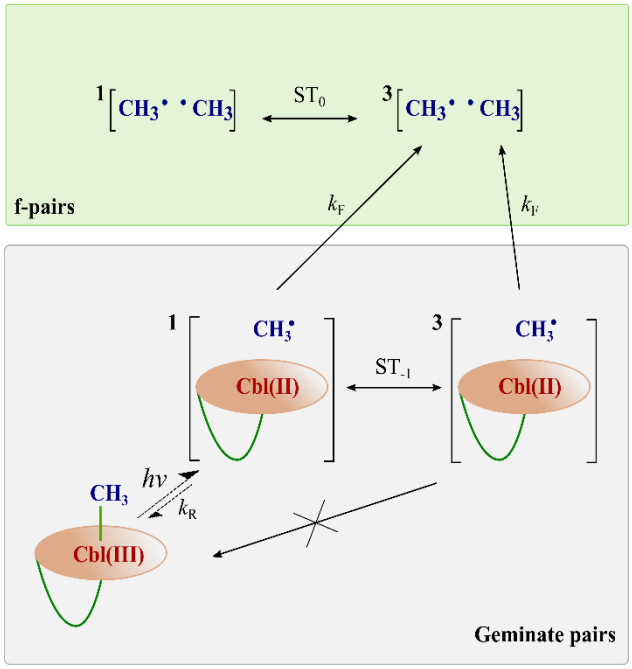

Figure 7. Schematic of the photochemical spin dynamics of MeCbl. The cobalamin (Cbl, orange oval and green loop) is simplified for clarity. See main text for full discussion. $h\upsilon$ - absorption of a photon resulting in homolysis; k_R – rate of RP recombination; ^{1}[ ] and ^{3}[ ] – singlet and triplet spin-states, respectively, of the RPs; ST_{-1} and ST_0 – the specific RP spin-states between which interconversion takes place generating spin polarization; k_F – rate of methyl radical diffusion to form methyl-methyl f-pairs. Various side reactions are possible for the methyl radical, including the S-born f-pairs recombining to form ethane (see main text for discussion), but these reaction channels have been left out of this figure for the sake of clarity.

The dominant role of the protein in tuning B_{12} reactivity appears to be borne out in the AdoCbl-dependent photoreceptor, CarH. Here, the main photochemical pathway avoids radical pairs altogether,[33, 53] despite the strong inclination of AdoCbl towards radical chemistry. That said, transient absorption data from the photolysis of MeCbl bound to methionine synthase suggests binding to the protein alone in the absence of substrate is not sufficient to significantly alter the photophysical branching and initial formation of the geminate RPs.[19] In MeCbl-dependent enzymes, therefore, it is highly likely that a combination of protein and substrate binding to the protein is required to guide MeCbl away from RP intermediates. This would be analogous to the fact that binding of AdoCbl to its dependent enzymes is not enough to weaken the Co–C bond to the upper axial ligand,[54] and that substrate binding is required to provide a 'trigger' for homolysis.[23, 25, 55-56]

EXPERIMETAL DETAILS

Materials

The following chemicals were purchased and used without further purification: MeCbl (methylcobalamin, Sigma), HEPES (Formedium Ltd), TEMPO (free radical, sublimed, ≥ 99%, Aldrich), glycerol (Merck), glucose (Sigma), and glucose oxidase (from *Aspergilus niger*,C Sigma). The triple-coated neodymium-iron-boron (NeFeB) permanent magnets were purchased from e-Magnetics UK. The 365 nm and 530 nm high-powered LEDs were purchased from ThorLabs.

Time resolved continuous flow EPR

All MeCbl sample solutions were prepared under red light in degassed aqueous 20 mM HEPES buffer with 0% or 50% glycerol w/w, pH 7.5. Buffers were filtered and degassed with nitrogen and stored in an anaerobic glove box (Belle Technology) for at least 24 h before sample preparation. The concentration of each sample was confirmed using a Cary 60 UV-Vis spectrophotometer (Agilent Technologies) using an extinction coefficient for MeCbl of $\varepsilon_{520\,nm} = 7.7\ mM^{-1}\ cm^{-1}$.[57] All sample vessels were stoppered with Suba-seals and sealed with parafilm to ensure retention of anaerobic conditions during transfer to the EPR spectrometer. Prior to and during EPR measurements samples were purged with Ar. FT-EPR experiments were performed on a Bruker ELEXSYS-500/580 X-band spectrometer using the pulsed mode with dielectric resonator (ER4118X-MD-5) and a home-built continuous flow setup (for further details refer to the Supporting Information, Section 1). Briefly, flow was achieved through the EPR cavity using a single piston HPLC Gilson 305 pump and a quartz EPR flow cell. The response of the sample to the microwave pulse was detected in quadrature using 4-step phase cycling routine. The second and third harmonic of a Brilliant blue B Nd:YAG laser (10 Hz) were used for excitation at 355 nm or 532 nm. The pulse energy at both wavelengths was attenuated to 20 mJ. Experiments were performed in triplicate, standard deviations are given in the Supporting Information.

Simulations

At thermal equilibrium, the hyperfine splitting pattern in the methyl radical EPR signal is expected to give four lines and an intensity pattern of 1:3:3:1. The transient spectra acquired shortly after photolysis of the Co-C bond in MeCbl, however, represent spin polarized states and the line intensities therefore

deviate from this pattern. In principle, such deviation can originate from one or more of various spin polarization mechanisms. The spin polarized signal of the methyl radical was therefore simulated for all possible spin polarization mechanisms for the methyl radical (Supporting info, Section 2 and Figure S2B). The negative hyperfine value for the methyl radical was taken into account. Stick spectra were generated for each of the standard CIDEP models presented in the Supporting Information, based on the computed density matrix elements, in order to calculate each of the intensity patterns. A Lorentzian line shape was then convoluted to the stick spectra to produce the simulated spectra presented. All code was written in Fortran and compiled and executed on a standard desktop PC. Lineshape convolution was performed using Igor Pro software.

Magnetic field effects

All MeCbl samples (~30 μM) were prepared in degassed, 20 mM HEPES/50% glycerol (w/w) pH 7.5 in a similar way to that described for the FT-EPR experiments. Glucose oxidase (13 units/mL) and glucose (10 mM) were added to all samples ~ 10 minutes prior to data acquisition to scavenge any residual oxygen. In similar, previously published MFE experiments with B_{12} cofactors,[24] TEMPO was added to a final concentration of 1 mM to selectively scavenge the alkyl radical. Data were acquired here both in the presence and absence of TEMPO to investigate whether or not it affects the magnitude of the MFE. It does not (Supporting Information, Figure S15).

Spectroscopic data were collected using a MFE stopped-flow spectrophotometer described previously,[58] and adapted to allow continuous wave photoexcitation at specific wavelengths. In these experiments, the continuous wave-photolysis of MeCbl was achieved by using high-power, fibre-coupled LEDs. Samples were exposed to light centred at either 365 nm or 530 nm and the accumulation of the cob(II)alamin radical was probed at 470 nm using the monochromated emission from a Xe arc lamp. Static MFs of ≈ 100 mT, which are sufficient to saturate the Zeeman effect of B_{12} RPs,[24] were generated by mounting pairs of NeFeB magnets in the unoccupied light-guide ports during data acquisition. Data were acquired at 25 °C over 100 s. Data from the first 4 stopped-flow shots were discarded because of the dead-volume between the syringes and the cell. Each experiment consisted of a set of 6 replicates of field on/field off pairs (the order of which was randomized).

ASSOCIATED CONTENT

Supporting Information is available containing supporting data and details of the experimental setup, spin dynamic simulations and kinetic calculations.

AUTHOR INFORMATION

Corresponding Author

*To whom correspondence should be addressed: alex.jones@npl.co.uk, A.J.Fielding@ljmu.ac.uk, woodward@global.c.u-tokyo.ac.jp

Author Contributions

The manuscript was written by ARJ and VL with contributions from all authors. All authors have given approval to the final version of the manuscript.

ACKNOWLEDGMENT

Funding Sources

VL and TM acknowledge Early Stage Research Funding from the European Union's seventh Framework Programme FP-7-PEOPLE-2013-ITN through the 'MAGnetic Innovation in Catalysis' (MAGIC) Initial Training Network (Grant agreement no.606831). We thank the National EPSRC EPR service and Facility (NS/A000055/1) for support. AJF thanks Bruker for sponsorship.

SUPPORTING INFORMATION AVAILABLE

The Supporting Information contains supplementary figures, methods and details of computer simulations. This information is available free of charge via the Internet at http://pubs.acs.org

ABBREVIATIONS

MeCbl, methylcobalamin; AdoCbl, 5'-deoxyadenosylcobalamin; RP, radical pair; FT-EPR, Fourier transform-electron paramagnetic resonance; CIDEP, chemically induced dynamic electron polarization; TM, triplet mechanism, TD-DFT, time-dependent density functional theory; S, singlet; T, triplet; DAF, delay-after-flash; RPM, radical pair mechanism; E/A, emission/absorption; MFE, magnetic field effects.

REFERENCES

1. Banerjee, R., *Chemistry and Biology of B12*. New York, Chichester, 1999.
2. Dali-Youcef, N.; Andrès, E., An update on cobalamin deficiency in adults. *QJM.* **2009,** *102* (1), 17-28.
3. Gruber, K.; Puffer, B.; Krautler, B., Vitamin B_{12}-derivatives-enzyme cofactors and ligands of proteins and nucleic acids. *Chem. Soc. Rev.* **2011,** *40* (8), 4346-4363.
4. Brown, K. L., Chemistry and enzymology of vitamin B_{12}. *Chem. Rev.* **2005,** *105*, 2075-2149.
5. Matthews, R. G.; Koutmos, M.; Datta, S., Cobalamin-dependent and cobamide-dependent methyltransferases. *Curr. Opin. Struct. Biol.* **2008,** *18* (6), 658-666.
6. Banerjee, R., Radical carbon skeleton rearrangements; catalysis by coenzyme B_{12}-dependent mutases. *Chem. Rev.* **2003,** *103* (6), 2083-2094.
7. Toraya, T., Radical catalysis in coenzyme B_{12}-dependent isomerization (eliminating) reactions. *Chem. Rev.* **2003,** *103*, 2095-2127.
8. Jones, A. R., The photochemistry and photobiology of vitmain B_{12}. *Photochem. Photobiol. Sci.* **2017,** *16* (6), 820-834.
9. Pratt, J. M., The chemistry of vitamin B_{12}. Part II. Photochemical reactions. *J. Chem. Soc.* **1964,** (0), 5154-5160.
10. Cole, A. G.; Yoder, L. M.; Shiang, J. J.; Anderson, N. A.; Walker, L. A.; Banaszak Holl, M. M.; Sension, R. J., Time-resolved spectroscopic studies of B_{12} coenzymes: a comparison of the primary photolysis mechanism in methyl-, ethyl-, n-propyl-, and 5'-deoxyadenosylcobalamin. *J. Am. Chem. Soc.* **2002,** *124* (3), 434-441.
11. Harris, D. A.; Stickrath, A. B.; Carroll, E. C.; Sension, R. J., Influence of environment on the electronic structure of cob(III)alamins: Time-resolved absorption studies of the S1 state spectrum and dynamics. *J. Am. Chem. Soc* **2007,** *129* (24), 7578-7585.
12. Miller, N. A.; Deb, A.; Alonso-Mori, R.; Garabato, B. D.; Glownia, J. M.; Kiefer, L. M.; Koralek, J.; Sikorski, M.; Spears, K. G.; Wiley, T. E., Polarized XANES monitors femtosecond structural evolution of photoexcited vitamin B_{12}. *J. Am. Chem. Soc* **2017,** *139* (5), 1894-1899.
13. Peng, J.; Tang, K.-C.; McLoughlin, K.; Yang, Y.; Forgach, D.; Sension, R. J., Ultrafast excited-state dynamics and photolysis in base-off B_{12} coenzymes and analogues: absence of the trans-nitrogenous ligand opens a channel for rapid nonradiative decay. *J. Phys. Chem. B* **2010,** *114* (38), 12398-12405.
14. Rury, A. S.; Wiley, T. E.; Sension, R. J., Energy cascades, excited state dynamics, and photochemistry in cob(III)alamins and ferric porphyrins. *Acc. Chem. Res.* **2015,** *48* (3), 860-867.

15. Sension, R. J.; Harris, D. A.; Cole, A. G., Time-resolved spectroscopic studies of B_{12} coenzymes: comparison of the influence of solvent on the primary photolysis mechanism and geminate recombination of methyl-, ethyl-, n-propyl-, and 5'-deoxyadenosylcobalamin. *J. Phys. Chem. B* **2005,** *109* (46), 21954-21962.
16. Shiang, J. J.; Cole, A. G.; Sension, R. J.; Hang, K.; Weng, Y.; Trommel, J. S.; Marzilli, L. G.; Lian, T., Ultrafast excited-state dynamics in vitamin B_{12} and related cob(III)alamins. *J. Am. Chem. Soc.* **2006,** *128* (3), 801-808.
17. Shiang, J. J.; Walker, L. A.; Anderson, N. A.; Cole, A. G.; Sension, R. J., Time-resolved spectroscopic studies of B_{12} coenzymes: the photolysis of methylcobalamin is wavelength dependent. *J. Phys. Chem. B* **1999,** *103* (47), 10532-10539.
18. Stickrath, A. B.; Carroll, E. C.; Dai, X.; Harris, D. A.; Rury, A.; Smith, B.; Tang, K.-C.; Wert, J.; Sension, R. J., Solvent-dependent cage dynamics of small nonpolar radicals: lessons from the photodissociation and geminate recombination of alkylcobalamins. *J. Phys. Chem. A* **2009,** *113* (30), 8513-8522.
19. Walker, L. A.; Jarrett, J. T.; Anderson, N. A.; Pullen, S. H.; Matthews, R. G.; Sension, R. J., Time-resolved spectroscopic studies of B_{12} coenzymes: the identification of a metastable cob(III)alamin photoproduct in the photolysis of methylcobalamin. *J. Am. Chem. Soc.* **1998,** *120* (15), 3597-3603.
20. Walker, L. A.; Shiang, J. J.; Anderson, N. A.; Pullen, S. H.; Sension, R. J., Time-resolved spectroscopic studies of B_{12} coenzymes: the photolysis and geminate recombination of adenosylcobalamin. *J. Am. Chem. Soc.* **1998,** *120* (29), 7286-7292.
21. Wiley, T. E.; Miller, W. R.; Miller, N. A.; Sension, R. J.; Lodowski, P.; Jaworska, M.; Kozlowski, P. M., Photostability of hydroxocobalamin: ultrafast excited state dynamics and computational studies. *J. Phys. Chem. Lett.* **2016,** *7* (1), 143-147.
22. Yoder, L. M.; Cole, A. G.; Walker, L. A.; Sension, R. J., Time-resolved spectroscopic studies of B_{12} coenzymes: influence of solvent on the photolysis of adenosylcobalamin. *J. Phys. Chem. B* **2001,** *105* (48), 12180-12188.
23. Jones, A. R.; Levy, C.; Hay, S.; Scrutton, N. S., Relating localized protein motions to the reaction coordinate in coenzyme B_{12}-dependent enzymes. *FEBS J.* **2013,** *280* (13), 2997-3008.
24. Jones, A. R.; Woodward, J. R.; Scrutton, N. S., Continuous wave photolysis magnetic field effect investigations with free and protein-bound alkylcobalamins. *J. Am. Chem. Soc.* **2009,** *131*, 17246-17253.
25. Jones, A. R.; Hardman, S. J. O.; Hay, S.; Scrutton, N. S., Is there a dynamic protein contribution to the substrate trigger in coenzyme B_{12}-dependent ethanolamine ammonia lyase? *Angew. Chem. Int. Ed.* **2011,** *50* (46), 10843-10846.
26. Sension, R. J.; Cole, A. G.; Harris, A. D.; Fox, C. C.; Woodbury, N. W.; Lin, S.; Marsh, E. N. G., Photolysis and recombination of adenosylcobalamin bound to glutamate mutase. *J. Am. Chem. Soc.* **2004,** *126* (6), 1598-1599.
27. Sension, R. J.; Harris, D. A.; Stickrath, A.; Cole, A. G.; Fox, C. C.; Marsh, E. N. G., Time-resolved measurements of the photolysis and recombination of adenosylcobalamin bound to glutamate mutase. *J. Phys. Chem. B* **2005,** *109* (38), 18146-18152.
28. Pérez-Marín, M. C.; Padmanabhan, S.; Polanco, M. C.; Murillo, F. J.; Elías-Arnanz, M., Vitamin B_{12} partners the CarH repressor to downregulate a photoinducible promoter in *Myxococcus xanthus*. *Mol. Microbiol.* **2008,** *67* (4), 804-819.
29. Ortiz-Guerrero, J. M.; Polanco, M. C.; Murillo, F. J.; Padmanabhan, S.; Elías-Arnanz, M., Light-dependent gene regulation by a coenzyme B_{12}-based photoreceptor. *Proc. Natl. Acad. Sci. USA* **2011,** *108* (18), 7565-7570.
30. Díez, A.; Ortiz-Guerrero, J.; Ortega, A.; Elías-Arnanz, M.; Padmanabhan, S.; García de la Torre, J., Analytical ultracentrifugation studies of oligomerization and DNA-binding of TtCarH, a *Thermus thermophilus* coenzyme B_{12}-based photosensory regulator. *Eur Biophys J* **2013,** *42* (6), 463-476.
31. Cheng, Z.; Li, K.; Hammad, L. A.; Karty, J. A.; Bauer, C. E., Vitamin B_{12} regulates photosystem gene expression via the CrtJ antirepressor AerR in *Rhodobacter capsulatus*. *Mol. Microbiol.* **2014,** *91* (4), 649-664.
32. Jost, M.; Fernández-Zapata, J.; Polanco, M. C.; Ortiz-Guerrero, J. M.; Chen, P. Y.-T.; Kang, G.; Padmanabhan, S.; Elías-Arnanz, M.; Drennan, C. L., Structural basis for gene regulation by a B_{12}-dependent photoreceptor. *Nature* **2015**.
33. Kutta, R. J.; Hardman, S. J. O.; Johannissen, L. O.; Bellina, B.; Messiha, H. L.; Ortiz-Guerrero, J. M.; Elias-Arnanz, M.; Padmanabhan, S.; Barran, P.; Scrutton, N. S., et al., The photochemical mechanism of a B_{12}-dependent photoreceptor protein. *Nat Commun* **2015,** *6*, 7907.
34. Cheng, Z.; Yamamoto, H.; Bauer, C. E., Cobalamin's (vitamin B_{12}) surprising function as a photoreceptor. *Trends Biochem. Sci.* **2016,** *41* (8), 647-650.
35. Padmanabhan, S.; Jost, M.; Drennan, C. L.; Elías-Arnanz, M., A new facet of vitamin B_{12}: gene regulation by cobalamin-based photoreceptors. *Annu. Rev. Biochem.* **2017,** *86* (1), 485-514.
36. Bussandri, A. P.; Kiarie, C. W.; Van Willigen, H., Photoinduced bond homolysis of B_{12} coenzymes, An FT-EPR study. *Res. Chem. Intermed.* **2002,** *28* (7-9), 697-710.
37. Chagovetz, A. M.; Grissom, C. B., Magnetic field effects in adenosylcob(III)alamin photolysis: relevance to B_{12} enzymes. *J. Am. Chem. Soc.* **1993,** *115*, 12152-12157.
38. Rao, D. N. R.; Symons, M. C. R., Effects of ionizing radiation and photolysis on methyl-cobalamin in low temperature matrices: an E.S.R. study. *J. Chem. Soc. Chem. Commun.* **1982,** (16), 954-955.
39. Sakaguchi, Y.; Hayashi, H.; I'Haya, Y. J., Fast formation of methyl radical from methylaquocobaloxime as studied by time-resolved optical and ESR techniques. *J. Phys. Chem.* **1990,** *94*, 291-293.
40. Jaworska, M.; Lodowski, P.; Andruniow, T.; Kozlowski, P. M., Photolysis of methylcobalamin: identification of the relevant excited states involved in Co-C bond scission. *J. Phys. Chem. B* **2007,** *111* (10), 2419-2422.
41. Lodowski, P.; Jaworska, M.; Andruniów, T.; Garabato, B. D.; Kozlowski, P. M., Mechanism of Co–C bond photolysis in the base-on form of methylcobalamin. *J. Phys. Chem. A* **2014,** *118* (50), 11718-11734.
42. Saraswat, R. S., Upretti, G.C. , Estimation of T1 of fast relaxing Co 2+ions from the observed EPR linewidth of Mn 2+ and VO 2+ impurities in some cobalt salt single crystals. *Phys. Stat. Sol.* **1978,** *87* (1), 39-42.
43. van Slageren, J.; Martino, D. M.; Kleverlaan, C. J.; Bussandri, A. P.; van Willigen, H.; Stufkens, D. J., FT-EPR Study of methyl radicals photogenerated from $[Ru(Me)(SnPh_3)(CO)_2(iPr\text{-}DAB)]$ and $[Pt(Me)_4(iPr\text{-}DAB)]$: an example of a strong excitation wavelength dependent CIDEP effect. *J. Phys. Chem. A* **2000,** *104* (25), 5969-5973.
44. Wong, S. K., Hutchinson, D.A., Wan, J.K.S., Chemically induced dynamic electron polarization. II. A general theory for radicals produced by photochemical reactions of excited triplet carbonyl compounds. *J. Chem. Phys.* **1973,** *58* (3), 985-989.
45. Atkins, P. W., Evans, G.T., Electron spin polarization in a rotating triplet. *Mol. Phys.* **1974,** *27* (6), 1633-1644.
46. Lodowski, P.; Jaworska, M.; AndrunioÃÅw, T.; Kumar, M.; Kozlowski, P. M., Photodissociation of Co-C Bond in methyl- and ethylcobalamin: An insight from TD-DFT calculations. *J. Phys. Chem. B* **2009,** *113* (19), 6898-6909.
47. Lodowski, P.; Jaworska, M.; Garabato, B. D.; Kozlowski, P. M., Mechanism of Co–C bond photolysis in methylcobalamin: influence of axial base. *J. Phys. Chem. A* **2015,** *119* (17), 3913-3928.
48. Andruniów, T.; Lodowski, P.; Garabato, B. D.; Jaworska, M.; Kozlowski, P. M., The role of spin-orbit coupling in the photolysis of methylcobalamin. *J. Chem. Phys.* **2016,** *144* (12), 124305.
49. Kainrath, S.; Stadler, M.; Reichhart, E.; Distel, M.; Janovjak, H., Green-light-induced inactivation of receptor signaling using cobalamin-binding domains. *Angew. Chem. Int. Ed.* **2017,** *56* (16), 4608-4611.
50. Chatelle, C.; Ochoa-Fernandez, R.; Engesser, R.; Schneider, N.; Beyer, H. M.; Jones, A. R.; Timmer, J.; Zurbriggen, M. D.; Weber, W., A green-light-responsive system for the control of transgene expression in mammalian and plant cells. *ACS Synth. Biol.* **2018,** *7* (5), 1349-1358.
51. Wang, R.; Yang, Z.; Luo, J.; Hsing, I.-M.; Sun, F., B_{12}-dependent photoresponsive protein hydrogels for controlled stem cell/protein release. *Proc. Natl. Acad. Sci. USA* **2017,** *114* (23), 5912-5917.
52. Lott, W. B.; Chagovetz, A. M.; Grissom, C. B., Alkyl radical geometry controls geminate cage recombination in alkylcobalamins. *J. Am. Chem. Soc.* **1995,** *117* (49), 12194-12201.

53. Jost, M.; Simpson, J. H.; Drennan, C. L., The transcription factor CarH safeguards use of adenosylcobalamin as a light sensor by altering the photolysis products. *Biochemistry* **2015,** *54* (21), 3231-3234.
54. Brooks, A. J.; Vlasie, M.; Banerjee, R.; Brunold, T. C., Spectroscopic and computational studies on the adenosylcobalamin-dependent methylmalonyl-CoA mutase evaluation of enzymatic contributions to Co-C bond activation in the Co^{3+} ground state. *J. Am. Chem. Soc.* **2004,** *126* (26), 8167-8180.
55. Chen, Z.-G.; Ziętek, M. A.; Russell, H. J.; Tait, S.; Hay, S.; Jones, A. R.; Scrutton, N. S., Dynamic, electrostatic model for the generation and control of high-energy radical intermediates by a coenzyme B_{12}-dependent enzyme. *ChemBioChem* **2013,** *14* (13), 1529-1533.
56. Russell, H. J.; Jones, A. R.; Hay, S.; Greetham, G. M.; Towrie, M.; Scrutton, N. S., Protein motions are coupled to the reaction chemistry in coenzyme B_{12}- dependent ethanolamine ammonia lyase. *Angew. Chem. Int. Ed.* **2012,** *51*, 9306-9310.
57. Hogenkamp, H. P. C., Holmes, S., Polarography of cobalamins and cobinamides. *Biochemistry* **1970,** *9* (9), 1886-1892.
58. Jones, A. R.; Scrutton, N. S.; Woodward, J. R., Magnetic field effects and radical pair mechanisms in enzymes: a reappraisal of the horseradish peroxidase system. *J. Am. Chem. Soc.* **2006,** *128*, 8408-8409.

TOC Graphic